Instituto Superior Técnico
DEPARTAMENTO DE FÍSICA
Av. Rovisco Pais, 1096 Lisboa Codex, Portugal

DF-IST-6-91

DF-IST-6-91
IST-DF-6/91

Elimination of Transverse Beam Instabilities in Accumulation Rings by Application of an External Periodic Force

R. Alves–Pires and **R. Dilão**

IST, Department of Physics, Av. Rovisco Pais, P-1096 Lisboa Codex, Portugal

Abstract

An efficient procedure for the elimination of transverse beam instabilities is derived using a simple model for the beam–ions interaction. The method consists in sweeping periodically the beam shaking frequency near the hysteresis associated to a strongly non–linear resonance. Efficient shaking is then obtained as arbitrarily large ion amplitudes can be induced.

ROUTE TO

NAME	LOCATION

RETURN TO ...

Classification: Physics of beams; PACS: 41.80.Gg, 07.77.+p, 29.25.Fb

1. Introduction

In the vacuum chamber of antiproton accumulation rings the interaction of beam particles with the residual gas produces positively charged ions which oscillate around the negatively charged beam. The presence of ions near the beam constrains the accumulation rate and the maximum number of accumulated antiprotons. To minimize this problem, Orlov and co-workers have proposed and implemented a method which consists in shaking the beam at fixed frequency, increasing the amplitude of ion oscillations in the transverse plane to the accumulation ring, [1], [5] and [6].

In this paper we derive the equation of motion for the ions of the residual gas under the action of the potential created by the beam of charged particles. The motion of the ions in the transverse plane is strongly non-linear and we study the changes in the dynamics introduced by an external periodic force — beam shaking.

We found a pattern of non-linear resonance known as hysteresis or jump bifurcation, where amplitude growth can only be reached by a suitable variation in a frequency parameter. Using this fact, we propose a new method to increase arbitrarily the amplitude of ion oscillations, leading to the increase of efficiency of particle accumulation.

It is found that the relevant parameter driving this amplitude growth is the ratio ω_0/ν, where ω_0 is the ion linear bouncing frequency and ν is the shaking frequency. So, the ion amplitude growth is forced by decreasing periodically the frequency ν. In Orlov's approach, where ν is kept fixed, the increase of the oscillation amplitude of the ions is due to the variation of ω_0, originated by their slow longitudinal motion [6].

Numerical simulations show a strong efficiency in the variable frequency shaking. We considered, in the vertical transverse direction to the vacuum chamber, a Gaussian distribution of ions with r.m.s. size σ. After 5 variable frequency shaking cycles, the r.m.s. size of the distribution of ions increases to 10σ.

2. Equation of the motion of the ions

We consider a beam of particles (antiprotons) as a cylindrical charge distribution $\rho(x, z, s)$, gaussian in the transverse plane and uniform in the longitudinal direction,

$$\rho\ (x, z, s) = \frac{\lambda}{2\pi\sigma^2}\ e^{-[(x-x_c)^2+(z-z_c)^2]/2\sigma^2}$$

where x and z denote the coordinates in the transverse plane, s is the coordinate along the longitudinal direction and λ is the longitudinal linear charge density; σ is the root mean square (r.m.s.) transverse size of the beam and (x_c, z_c) the location of the centre of the beam.

The charge distribution $\rho(x, z, s)$ generates a radial electric field $E_r(r)$ which can be easily computed using Gauss' theorem. In cylindric coordinates,

$$\frac{1}{r}\frac{\partial}{\partial r}(rE_r(r)) = \frac{\rho(r)}{\varepsilon_0} = \frac{\lambda}{2\pi\varepsilon_0\sigma^2}e^{-r^2/2\sigma^2},$$

where $r = \sqrt{(x - x_c)^2 + (z - z_c)^2}$.

The solution for the radial electric field is

$$E_r(r) = \frac{\lambda}{2\pi\varepsilon_0}\frac{1 - e^{-r^2/2\sigma^2}}{r} = \frac{\lambda}{2\pi\varepsilon_0}\left(\frac{r}{2\sigma^2} - \frac{r^3}{8\sigma^4} + \ldots\right) \tag{2.1}$$

and can be derived from the potential

$$V(r) = -\int_0^r E_r(r)dr = -\frac{\lambda}{2\pi\varepsilon_0}\int_0^r \frac{1 - e^{-r^2/2\sigma^2}}{r}dr = -\frac{\lambda}{4\pi\varepsilon_0}\int_0^{r^2/2\sigma^2}\frac{1 - e^{-u}}{u}du\,.$$

Collision of beam particles with the atoms of the residual gas produce ions that begin to move under the action of the potential created by the beam. In the transverse plane to the vacuum chamber, the ions move under the action of the force generated by the radial electric field (2.1).

We now consider an external oscillating electric field with frequency ν applied vertically to the beam — beam shaking. Under the action of the external field the beam oscillates around the design orbit with an amplitude z_0: $z_c(t) = z_0 \sin(\nu t)$. We suppose that the amplitude z_0 is small when compared with the beam r.m.s. size σ in such a way that the stability of the beam is not affected. We further assume that the electric field generated by the beam is the same as in the static case.

As the shaking perturbation is vertical, we study the motion of the ions along the vertical direction, neglecting coupling effects, as for example the magnetostatic field generated by the beam charge density $\rho(x, z, s)$. Thus, the Lorentz equation for the motion of an ion with mass m and electric charge q is,

$$m\ddot{z} = qE_z(x_c, z)$$

Using (2.1) to compute E_z we obtain,

$$m\ddot{z} = \frac{q\lambda}{2\pi\varepsilon_0}\frac{1 - e^{-[z - z_c(t)]^2/2\sigma^2}}{z - z_c(t)}$$

where $q\lambda < 0$ (the beam and the ions have opposite charges).

Defining a new normalized variable $y = (z - z_c(t))/2\sigma = (z - z_0\sin(\nu t))/2\sigma$, we reduce the above equation to the form

$$\ddot{y} + \omega_0^2\frac{1 - e^{-2y^2}}{2y} = \nu^2 A\sin(\nu t) \tag{2.2}$$

where $A = z_0/2\sigma$ is the amplitude of the external forcing (small parameter) and the linear bouncing frequency ω_0 of the ions is

$$\omega_0 = \sqrt{\frac{-q\lambda}{4\pi\varepsilon_0 m\sigma^2}} = \sqrt{\frac{|q\lambda|}{4\pi\varepsilon_0 m\sigma^2}} \ . \tag{2.3}$$

Equation (2.2) describes the motion of an ion in the field of the shaken beam.

In the absence of shaking, the right-hand side of equation (2.2) is zero and $y = z/2\sigma$. So, the phase space structure is easily derived, since the orbits in phase space are solutions of the Hamiltonian

$$H = \frac{\dot{y}^2}{2} + \frac{\omega_0^2}{4}\int_0^{2y^2} \frac{1-e^{-u}}{u} du = \text{constant} \ . \tag{2.4}$$

The orbits in phase space associated to the Hamiltonian (2.4) are closed curves corresponding to oscillatory motion of the ions around the centre of the beam, figure 1a). However, these oscillations are non–linear and the frequency of oscillation depends on the amplitude, figure 1b). For very small amplitudes, the non–linear term in equation (2.2) is

$$\omega_0^2 \ \frac{1-e^{-2y^2}}{2y} = \omega_0^2 \ (y - y^3 + \frac{2}{3}y^5 + \dots \ ) \tag{2.5}$$

and, near the origin, the ions oscillate with frequency ω_0. The frequency of oscillations decreases as the amplitude increases.

In the next section we develop a perturbative method, based on the Bogoliubov-Krylov averaging theory [3] and [4], to study the small amplitude solutions of the non–linear equation (2.2).

3. Resonance analysis

We first write (2.2) in the form

$$\ddot{y} + \omega_0^2 \ y = f(y) + \nu^2 A \sin(\nu t) \tag{3.1}$$

where

$$f(y) = \omega_0^2\Big(y - \frac{1-e^{-2y^2}}{2y}\Big) = \omega_0^2 \ \Big(y^3 - \frac{2}{3}y^5 + \dots \Big) \tag{3.2}$$

and we look for oscillating solutions with frequency ν near ω_0.

As $f(y)$ goes to zero as y^3 and A is assumed small, we expect particular solutions of (3.1) of harmonic type, with, eventually, a time dependent amplitude $a(t)$ and phase $\theta(t)$. Therefore, we write the solutions of (3.1) in the form

$$y = a(t)\cos(\nu t + \theta(t)) \tag{3.3a}$$

$$\dot{y} = -\nu a(t)\sin(\nu t + \theta(t)) \tag{3.3b}$$

Consistency in the solutions (3.3) implies that the derivative of (3.3a) be equal to (3.3b), leading to the equation

$$\frac{da}{dt}\cos(\nu t+\theta) - a\frac{d\theta}{dt}\sin(\nu t+\theta) = 0 \ . \tag{3.4}$$

Derivation of (3.3b) and introduction in (3.1) gives

$$\begin{aligned}\nu\frac{da}{dt}\sin(\nu t+\theta)+a\nu\frac{d\theta}{dt}\cos(\nu t+\theta)& \\ = a\,(\omega_0^2-\nu^2)\cos(\nu t+\theta) - f(a\cos(\nu t+\theta)) + \nu^2 A\sin(\nu t+\theta)\ .&\end{aligned} \tag{3.5}$$

Solving (3.4) and (3.5) in order to $\dot{a}$ and $\dot{\theta}$, we obtain, for the unknown amplitude and phase, the system of differential equations:

$$\begin{aligned}\dot{a} &= \frac{1}{\nu}\Big((\omega_0^2-\nu^2)a\cos\gamma - f(a\cos\gamma) - \nu^2 A\sin(\nu t)\Big)\sin\gamma \\ \dot{\theta} &= \frac{1}{a\nu}\Big((\omega_0^2-\nu^2)a\cos\gamma - f(a\cos\gamma) - \nu^2 A\sin(\nu t)\Big)\cos\gamma\end{aligned} \tag{3.6}$$

where $\gamma = \nu t + \theta$.

As we want to obtain information on the behavior of the system for time scales $t >> 2\pi/\nu$ we average the right-hand side of (3.6) over the period $2\pi/\nu$. Supposing that a and θ are constants in the right-hand side of (3.6), we obtain the system

$$\begin{aligned}\dot{a} &= -\frac{\nu A}{2}\cos\theta \\ \dot{\theta} &= -\frac{\nu}{2} + \frac{\nu A}{2a}\sin\theta + \frac{\omega_0^2}{2\nu}G(a^2)\end{aligned} \tag{3.7}$$

where

$$G(a^2) = \frac{1-e^{-a^2}I_0(a^2)}{a^2} \tag{3.8}$$

and $I_0(z)$ is a modified Bessel function of order zero.

In the long time behaviour, the phase trajectories of the Poincaré map of (3.1) are approximated by the continuous curves obtained as solutions of (3.7), [2]. With the new variables $u = a\cos\theta$ and $v = a\sin\theta$, we have, by inversion of (3.3),

$$\begin{aligned}u &= a\cos\theta = y\cos(\nu t) - \frac{\dot{y}}{\nu}\sin(\nu t) \\ v &= a\sin\theta = -y\sin(\nu t) - \frac{\dot{y}}{\nu}\cos(\nu t)\end{aligned} \tag{3.9}$$

In figure 2 we present the Poincaré map of (3.1) and the phase trajectories of (3.7) in the coordinates (3.9), for several values of the parameters. A good agreement is seen in

the neighborhood of the origin. This comparison legitimates our perturbative approach in this region. Far from the origin, the system (3.1) shows chaotic behavior and higher order resonances not described by (3.7) appear.

Fixed points of system (3.7) are special solutions of system (3.1). The equilibrium amplitude and phase of particular solutions of (3.1) are the fixed points of (3.7). So, the equilibrium amplitude and phase are given by

$$\cos\theta = 0$$
$$\frac{\omega_0^2}{\nu^2} G(a^2) = 1 - \frac{A}{a}\sin\theta \ .$$

from which we can compute the equilibrium amplitude as a function of the excitation frequency ν. Introducing the first condition into the second, we obtain

$$\frac{\omega_0}{\nu} = \sqrt{\frac{1 \mp A/a}{G(a^2)}} \ . \tag{3.10}$$

Relation (3.10) defines implicitly the value of the amplitude of a particular oscillatory solution of the non-linear system (3.1), as a function of the ratio ω_0/ν. Solving (3.10) with respect to ν and with $A = 0$, we obtain the frequency of the non-linear system as a function of the amplitude — black squares in figure 1.b).

Figure 3 shows the equilibrium amplitude a of the ion oscillations as a function of ω_0/ν, for various values of the amplitude of the external field A. However, not all the amplitudes are stable. Their stability is calculated from the Jacobian of (3.7) at the equilibrium values. In figure 3, stable equilibrium amplitudes are represented by heavy lines and unstable amplitudes by dotted lines. For the shaking frequency $\nu = \omega_0$, the long time solution of (3.1) has periodic behavior with amplitude $a(\nu)$. If we decrease adiabatically the shaking frequency ν the amplitude of oscillations increases.

The curves given by (3.10) define two regions where solutions of equation (3.1) are qualitatively different. We have either one or three equilibrium amplitudes separated by a transition value (TV). If the beam is shaken at a frequency such that the ratio ω_0/ν is below TV, the ions oscillate with a small amplitude; if the ratio ω_0/ν is above TV the ions can have stable oscillations with either a small or a large amplitude, depending on the initial conditions.

Therefore, keeping the ion linear bouncing frequency ω_0 fixed and decreasing the ratio ω_0/ν adiabatically from a value above TV, the amplitude of the ions experiences a small jump at TV — hysteresis or jump bifurcation. If we begin with a value ω_0/ν below TV and increase adiabatically the ratio ω_0/ν there is a continuous increase of the amplitude of the ions.

As the ions are produced near the centre of the beam they have initially small amplitudes of oscillation. If we consider an initial shaking frequency $\nu = \nu_1 > \omega_0$ ($\omega_0/\nu_1 < 1$) we can drive the amplitude growth of the ions by decreasing adiabatically ν to values $\omega_0/\nu_2 > TV$, following the higher curve in figure 3. Imposing a periodic decrease of the shaking frequency the ions are pumped from small to higher amplitudes.

We claim that this procedure of variable shaking frequency, or frequency pumping, is more efficient than the one currently used in accumulation rings, [5] and [6]. In fact, arbitrarily large ion amplitudes can be induced, by suitably choosing the ratios ω_0/ν_1 and ω_0/ν_2. This technique of frequency pumping amplifies the effects of the longitudinal adiabatic frequency drift proposed by Orlov.

To test numerically this procedure, we considered a Gaussian distribution of 1000 particles and we followed their trajectories during 2000 shaking periods ($t = 2000 \times 2\pi/\nu_1$). We changed periodically and linearly the shaking frequency from $\nu_1 = 1.4\omega_0$ to $\nu_2 = 0.57\omega_0$ during the time $400 \times 2\pi/\nu_1$. So, we have observed the evolution of the residual ions during 5 variable shaking periods. Figure 4 shows the final distribution of the particles in phase and real space after frequency pumping. The particle distribution has initial r.m.s. size σ and, after variable frequency shaking ,evolved to a configuration with r.m.s. size 10σ.

Keeping the shaking frequency ν fixed, the longitudinal adiabatic motion of the ions induces variations of the ratio ω_0/ν. In accumulation rings, where the beta function is not strongly variable, the fixed shaking frequency increases only slightly the amplitude of oscillation of the ions, as ω_0 varies as the inverse of the square root of the accelerator beta function. For the Antiproton Accumulator at CERN, the ratio between the minimum and the maximum values of ω_0 is approximately one half [6] and, by (3.10), the amplitude of the ions can increase at most to 3.5σ. So the fixed shaking frequency is not as efficient as the variable frequency shaking.

If the longitudinal motion of ions is slow they are trapped in the beam line between consecutive dipoles. In fact, if the cyclotron radius for longitudinal ion motion is small, that is, the ions have small longitudinal momentum, ions are scattered near the dipoles and they oscillate in the longitudinal direction between them. In this case, shaking at fixed frequency produces no significant increase in ion amplitudes whereas our method is as efficient as in other situations.

Finally, we would like to remark that the method we propose must be combined with cooling devices to avoid beam heating during the crossing of beam resonance bands.

Acknowledgement: One of us (R. A-P.) would like to acknowledge Y. Orlov and D. Möhl for the many enlightening discussions on beam shaking.

Bibliography

[1] R. Alves Pires, D. Möhl, Y. Orlov, F. Pedersen, A. Poncet and S. van der Meer, "On the theory of coherent instabilities due to coupling between a dense cooled beam and charged particles from the residual gas", Proceedings of the 1989 Particle Accelerator Conference, Chicago, p. 800-802 (IEEE Conf. Series), F. Bennett and J. Kopta ed., New York, 1990.

[2] J. Guckenheimer and P. J. Holmes, Nonlinear Oscillations, Dynamical Systems and Bifurcations of Vector Fields, Springer-Verlag, New-York, 1983.

[3] J. K. Hale,"Ordinary differential equations", Wiley, New York, 1969.

[4] N. Krylov and N. Bogoliubov, "Introduction to non–linear mechanics", Princeton University Press, Princeton, 1947.

[5] J. Marriner, D. Möhl, Y. Orlov, A. Poncet and S. van der Meer, "Experiments and practise in beam shaking", Particle Accelerators **30** (1990) 13-20.

[6] Y. Orlov, "The suppression of transverse instabilities caused by trapped ions in the AA by shaking of the $\bar{p}$ beam", Proceedings of the Workshop on Crystalline Ion Beams, p. 133-139, R. W. Hasse, I. Hofmann and D. Liesen ed., Darmstadt, 1989.

Note added in proof: Since the restricted circulation of this paper, P. Zhou and J. Rosenzweig implemented the techniques developed here for the theoretical analysis of cyclotron shaking: P. Zhou and J. Rosenzweig, "Ion clearing using cyclotron shaking", Proceedings of the Fermilab III Instabilities Workshop, June 1990, p. 39-50, S. Peggs and M. Harvey ed., Fermilab TM-1696.

Figure captions:

Figure 1: a) Phase space orbits of an ion in the non-linear field of a continuous beam — (2.4). b) Frequency of ions oscillation as a function of the phase space initial amplitude $(y, 0)$. Black squares denote predicted values for $A = 0$, according to (3.10).

Figure 2: Poincaré map of equation (3.1) (top) and phase curves of the averaged system (3.7) in the coordinates (u,v) defined by (3.9). a) $\omega_0/\nu = 0.9$ and $A = 0.05$; b) $\omega_0/\nu = 1.2$ and $A = 0.05$. Numerical integration has been performed with the Bulirsh-Stoer method.

Figure 3: Amplitude solutions of equation (3.1) as a function of the ratio ω_0/ν. Solid lines represent stable amplitude solution. Dotted lines, unstable amplitude solutions. If the ratio ω_0/ν decreases from a value above the transition value (TV) we observe a jump in the amplitude. If the ratio ω_0/ν increases from a value below TV, the variation of amplitude is always continuous. (Hysteresis phenomenon or jump bifurcation).

Figure 4: Phase space (top) and transverse vertical distribution of 1000 particles after 2000 shaking cycles. We show the initial distribution of particles (dashed) versus the final distribution. In the top figure the circle encloses the initial distribution of particles and in the bottom the dashed area is its transverse Gaussian distribution with initial r.m.s. size σ. After 5 variable shaking cycles the r.m.s. size of the final particle distribution is 10σ.

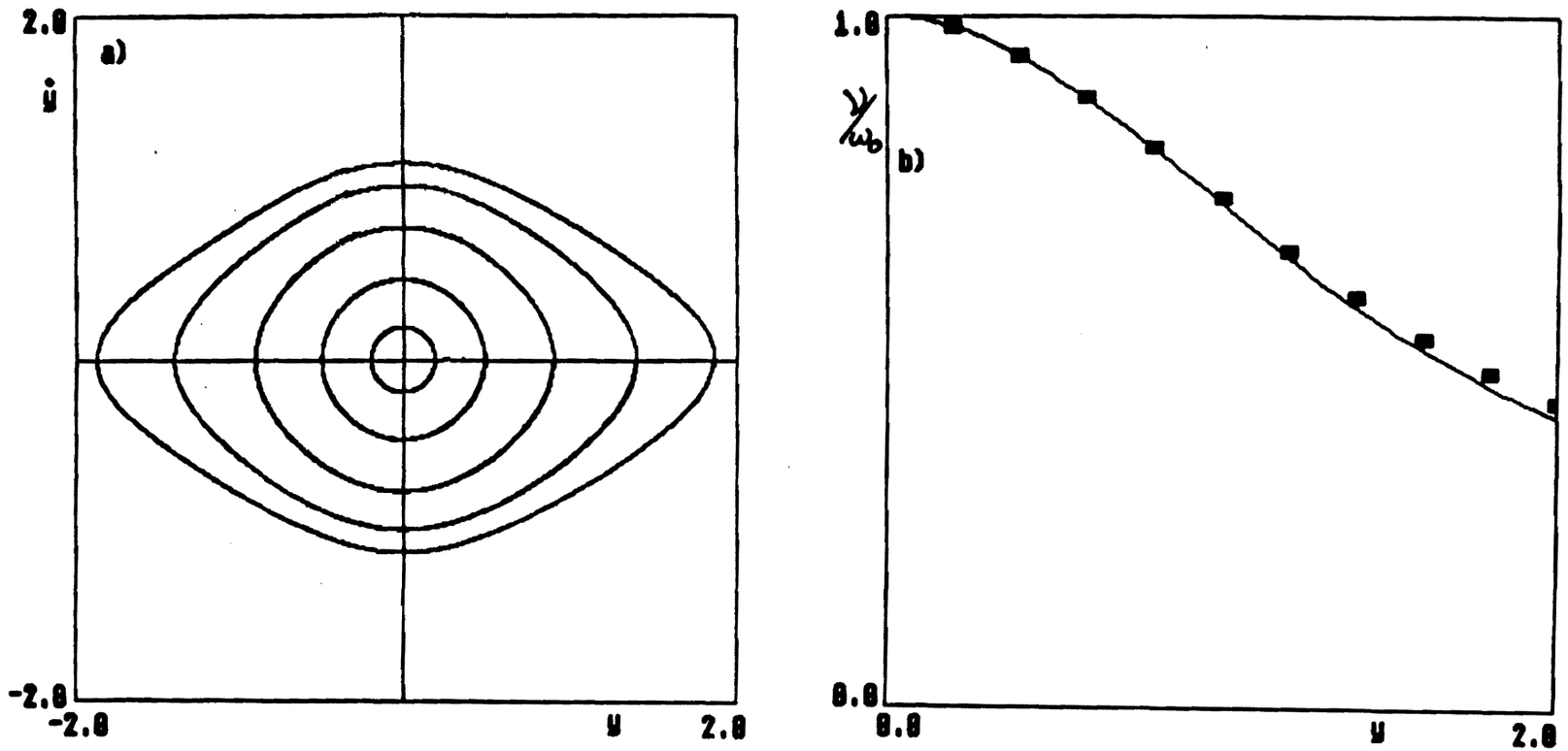

Figure 1

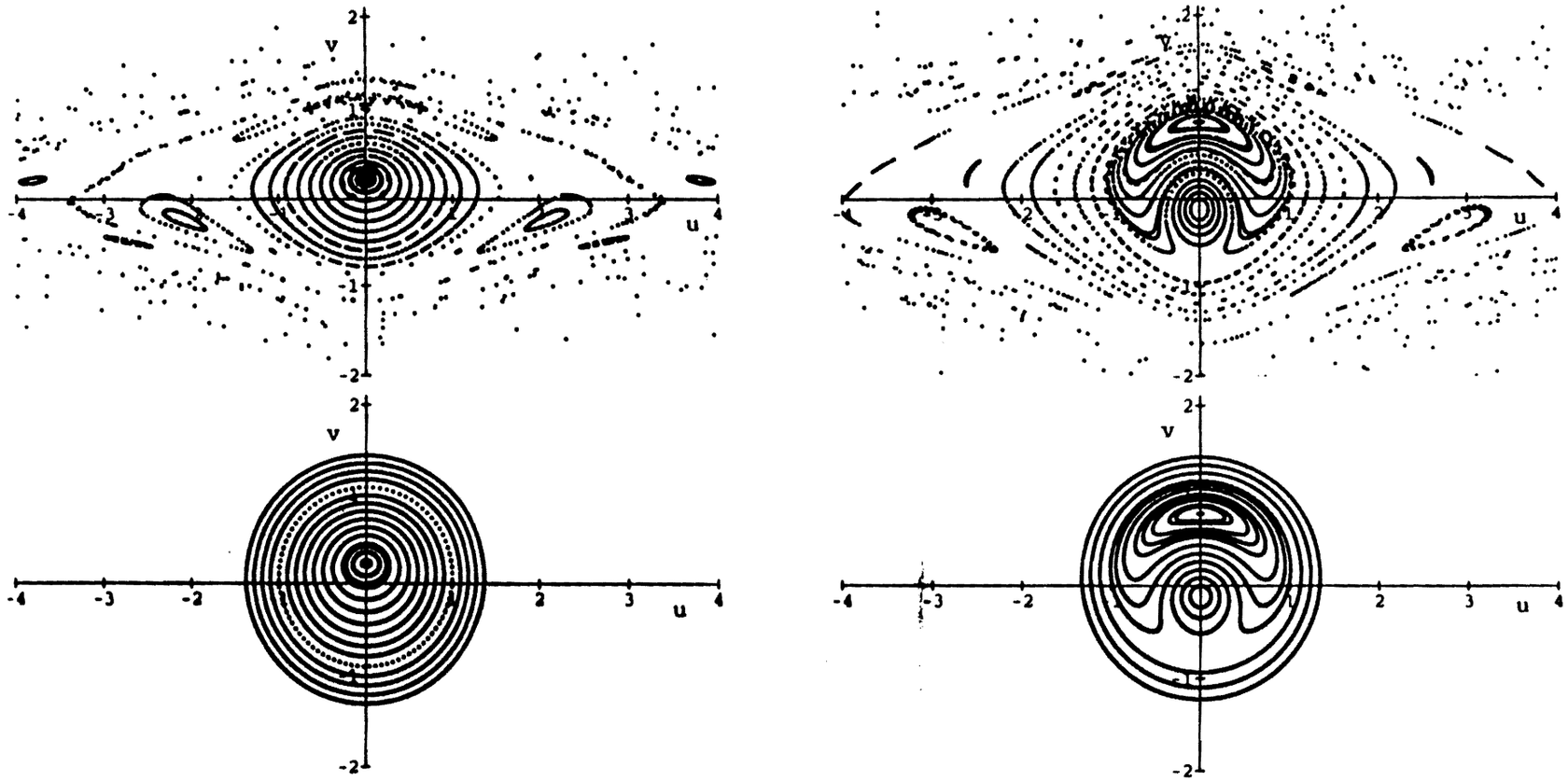

a) b)

Figure 2

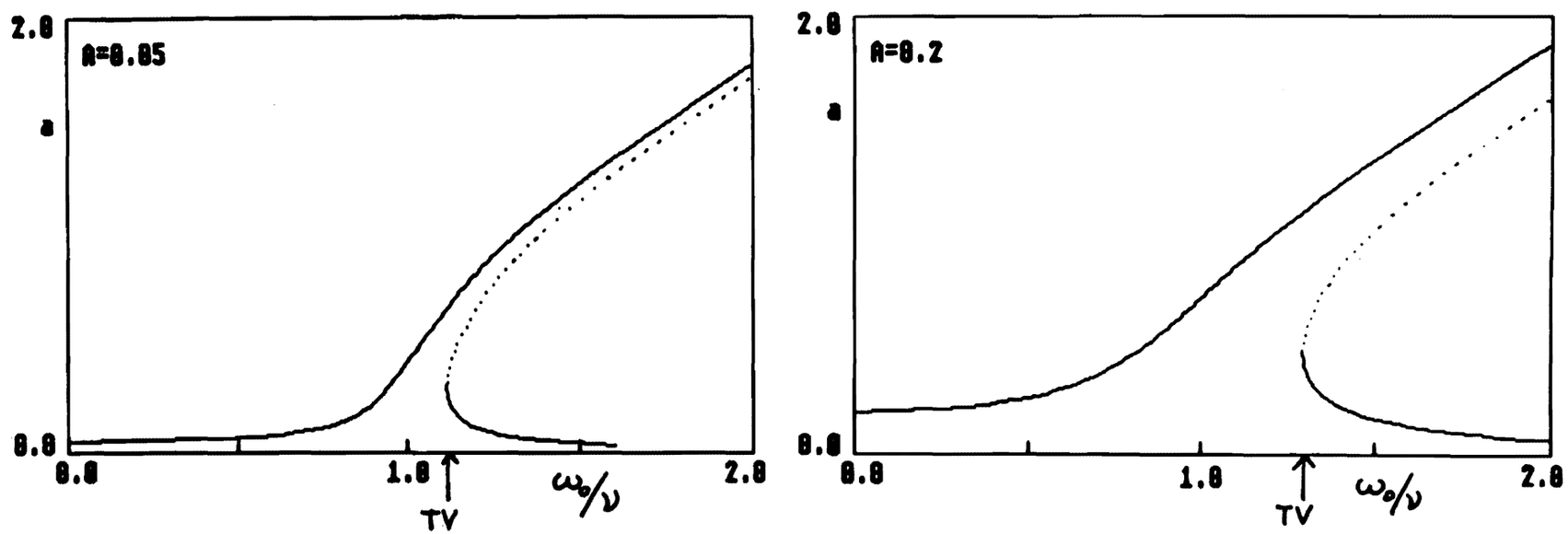

Figure 3

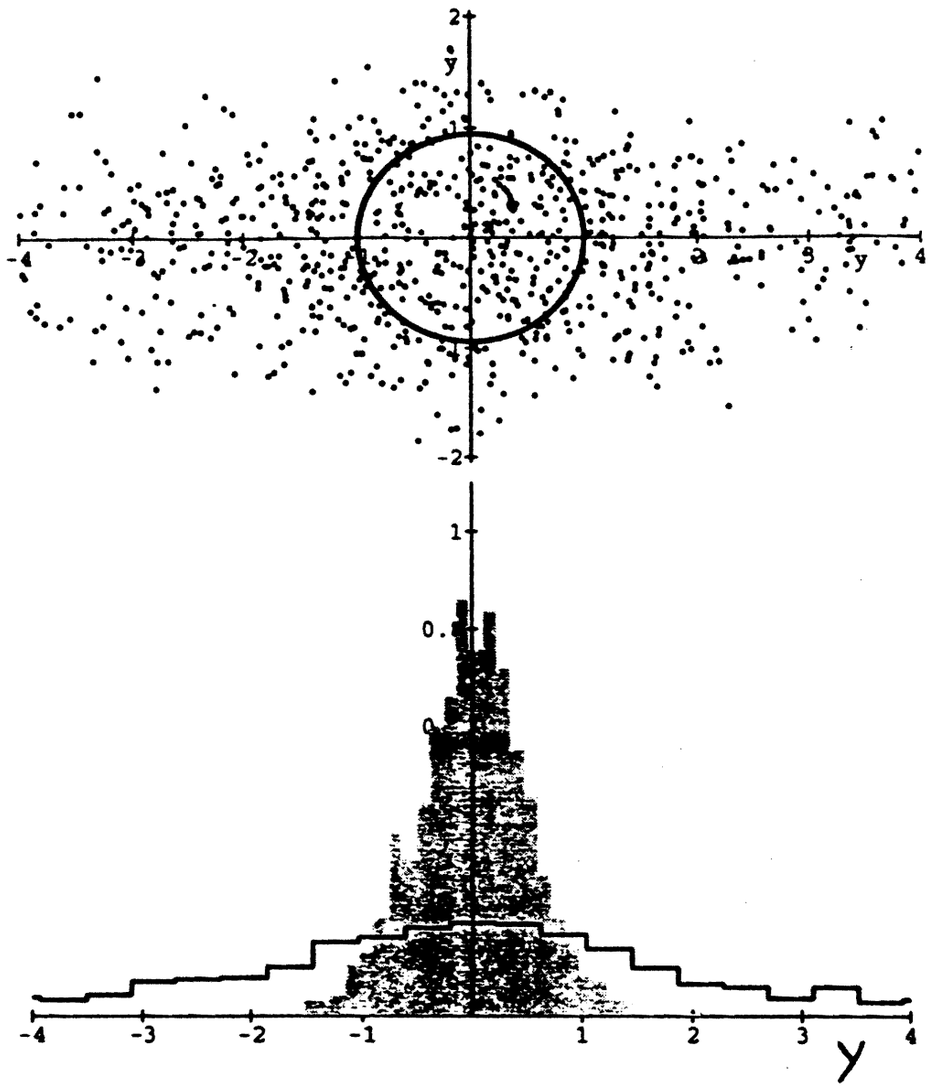

Figure 4